

Effect of applying ultrasonic vibration in thermal nanoimprint lithography

Harutaka Mekaru · Toshihiko Noguchi · Hiroshi Goto · Masaharu Takahashi

Received: 26 June 2007 / Accepted: 10 December 2007 / Published online: 9 January 2008
© Springer-Verlag 2007

Abstract In our previous works we had shown that the use of ultrasonic vibration in micro hot embossing processes proved to be effective in improving the molding accuracy. We then decided to extend this technology of ultrasonic vibration to nanoimprint lithography also, and investigate its effect on nanoimprints experimentally. This task also required the use of a heater capable of sustaining three kinds of stresses, namely loading force, thermal stress, and ultrasonic vibration in the molding process. This work led to the development of an ultrasonic nanoimprint system with a built-in pyrolytic graphite/pyrolytic boron nitride all-in-one heater. The material chosen for nanoimprinting was polycarbonate with its glass transition temperature being 150°C. The research in the area showed that the timing point at which an impression of ultrasonic vibration begins is an important factor. When an ultrasonic vibration was impressed at an early stage in a molding process the height of the imprinted pattern seemed to increase where high amplitudes of the acoustical vibration were involved. Moreover, when the molding accuracies of line/space pattern with line widths of 500, 750 nm, and 1 μm were compared among themselves, the effect of assistance from ultrasonic vibration became quite noticeable in the case of small lines patterns; this was the case even where the amplitudes of the ultrasonic vibration were small. As for the application of ultrasonic vibration on

nanoimprinting is concerned, it was found to greatly improve the molding accuracy of the process.

1 Introduction

As small and multifunctional electronic devices are being developed the need for high precision and cost effective micro parts is growing. LIGA process (Becker et al. 1986) is one such technology that can meet this need. The process employs X-ray lithography to make a resist structure that is then used in the fabrication of a mold using electroforming technology; the electroformed mold is then used for its final molding applications. A high sensitivity resist material SU-8 capable of thick film application was developed (Lorenz et al. 1998) that made it possible to make resist structure with high aspect ratios. With the help of such a technological development, pattern on the electroformed mold could be created with very high aspect ratios, although that also made the molding process more demanding and difficult. The difficulty that is encountered in the process relates to incomplete filling of melted thermoplastic material into mold's features with high aspect ratios resulting in poor and imprecise printing of features for the final product; the melting of the thermoplastic material is caused by the heating of the material which is a part of the over all operation. To solve this difficulty we tried impressing ultrasonic vibration on to the molding process which seemed to solve the problem of insufficient flow of the material into the mold features. We have already shown that it is effective to mold by impressing ultrasonic vibration at low loading force and short contact time in atmospheric hot embossing (Mekaru et al. 2007). In this experiment, an ultrasonic vibration of longitudinal

H. Mekaru (✉) · T. Noguchi · H. Goto · M. Takahashi
Advanced Manufacturing Research Institute, National Institute of Advanced Industrial Science and Technology, 1-2-1 Namiki, Tsukuba, Ibaraki 3058564, Japan
e-mail: h-mekaru@aist.go.jp

H. Goto
Micro-Pattern Imprinting Machine Division, Toshiba Machine Co. Ltd, 2068-3 Ooka, Numazu, Shizuoka 4108510, Japan

wave with the maximum amplitude of $18\ \mu\text{m}$ was impressed in a direction perpendicular to the mold pattern with its line widths ranging from $100\ \mu\text{m}$ to $1\ \text{mm}$. In another experiment same mold was used on a different molding system where the maximum amplitude was $1.8\ \mu\text{m}$ where in that case it showed that the amount of gas and air that had remained in the pattern decreased, and that the melted thermoplastic flowed quite adequately into the central region of the molding pattern (Mekaru et al. 2006). In the case where ultrasonic vibration was impressed during a molding process the impact of assistance of the ultrasonic process was found to be more effective where smaller size patterns with high aspect ratio features were involved. We then decided to combine thermal nanoimprint lithography (thermal-NIL) technology (Chou et al. 1995) with ultrasonic vibration.

The thermal-NIL technology was proposed by S.Y. Chou in 1995. This technology had already been applied in the fabrication of storage media such as compact-disc and a digital-versatile-disc. A system that integrates an ultrasonic vibration generator with a thermal-NIL system has already been developed at National Institute of Advanced Industrial Science and Technology (Kishi et al. 2003). Originally, the ultrasonic vibration was employed with an intention to ease the release of mold from the imprinted material during the demolding step (Maeda and Ashida 2004). Besides, the ultrasonic process was also considered as a useful technique for improving the molding process. This presumption led us to do a major restructuring and remodeling of the existing ultrasonic nanoimprint lithography (ultrasonic-NIL) system. The design required the use of a heater installed on the upper section of the system that could be used for the heating of mold. An important requirement associated with the heater was that it must be capable of sustaining triple stresses simultaneously, namely loading force, thermal stress, and ultrasonic vibration. Therefore, it was necessary to change to a special heater

with adequate mechanical strength. Using this improved thermal-NIL system, nanoimprint experiments were executed on a polycarbonate (PC) sheet where the effect of the assistance of ultrasonic vibration was experimentally confirmed. The Si mold with line/space patterns (line widths: 500 , $750\ \text{nm}$, and $1\ \mu\text{m}$) employed for this experiment was made using micro-electro-mechanical-system (MEMS) fabrication technology.

2 Preparation for experiments

2.1 Remodeling of ultrasonic nanoimprint lithography system

Figure 1 shows a photograph along with specifications of the ultrasonic-NIL system used for the experiment. Besides its main body this setup is also equipped with a coolant chiller sub-system for cooling. All operations for the system are controlled with a personal computer shown in the figure. Two loading stages are installed in the central part of the main body. As in a usual configuration, a mold is fixed to the upper loading stage and a thermoplastic sheet is put on the bottom loading stage. The mold can be heated up to a maximum temperature of 200°C , and be subjected to a maximum loading force of $5\ \text{kN}$. The upper loading stage can be moved in the direction of X axis by a linear motor and in the direction of Z axis by a servomotor (Fig. 1). Moreover, the bottom loading stage can be moved in the direction of Y axis by another linear motor, and rotated in the side of $\pm 3^\circ$ by another servomotor. By using step and stamp method, that employs these functions, a thermoplastic sheet of $200\ \text{mm} \times 100\ \text{mm}$, or less, can be imprinted. Figure 2a shows an internal structure of the upper loading stage. The heating system with a pyrolytic graphite (PG) ceramic heater and the cooling system by a thermal

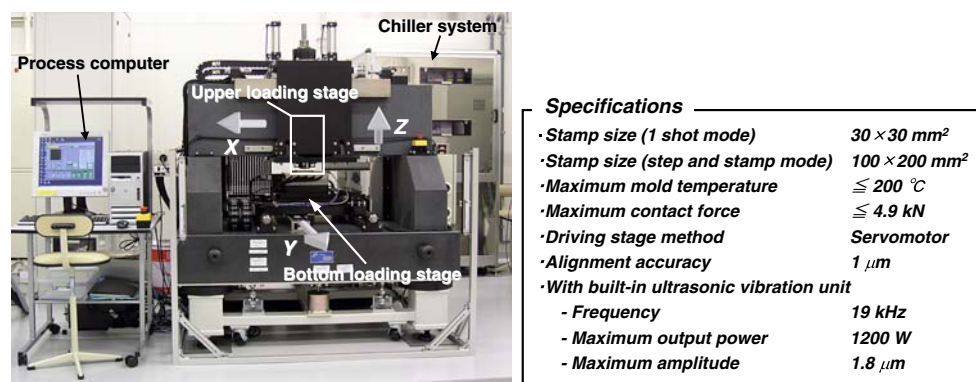
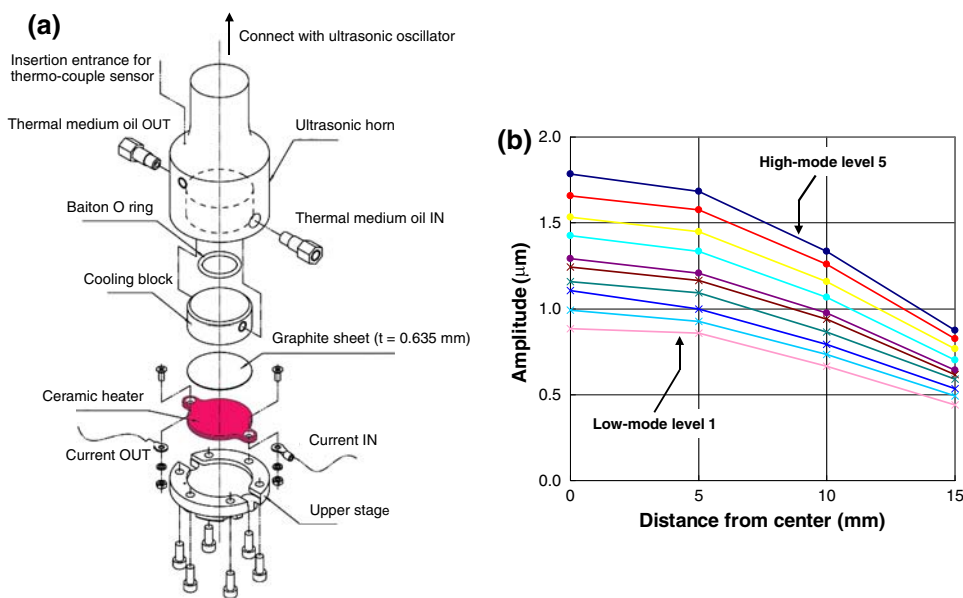


Fig. 1 Photograph and specifications of ultrasonic-NIL system. The upper loading stage is shown with a white frame

Fig. 2 a Internal structure of the upper loading stage in ultrasonic-NIL system. **b** Amplitude distribution on the upper loading stages



medium oil were mounted on the upper loading stage. In addition, a piezoelectric-type ultrasonic generator of a frequency 19 kHz and a maximum output power 1,200 W was installed in the upper part. The amplitude of the ultrasonic vibration can be changed in stages up to ten settings using the controller. Figure 2b shows the measurement results in terms of the amplitude of the ultrasonic vibration as function of the distance from the center of the upper loading stage. The ultrasonic vibration of the maximum amplitude of 0.8 µm is generated in controller's low-mode level 1, and the amplitude of 1.8 µm can be generated in high-mode level 5. The same cooling mechanism and the graphite heating system as on the upper loading stage were built into bottom loading stage.

By the way, impressing the ultrasonic vibration in the molding process amounts to three stresses namely loading force, thermal stress, and ultrasonic vibration simultaneously applied to the upper heater. These stresses often result in disengagement and disconnect of PG ceramic heating resistor in the upper stage. Figure 3a is a photograph of a disconnected PG heater. The PG heater was insulated electrically by a pyrolytic boron nitride (PBN) case. We thought that the cause of the disconnection was an insulation failure with the PBN ceramic case, and therefore we changed this to a PG/PBN heater (KH12190, GE Advanced Ceramics Corp.) in which the PG ceramic heater was completely covered by the PBN ceramic shown in Fig. 3b. Moreover, because we thought that the impression of the ultrasonic vibration at the precise timing

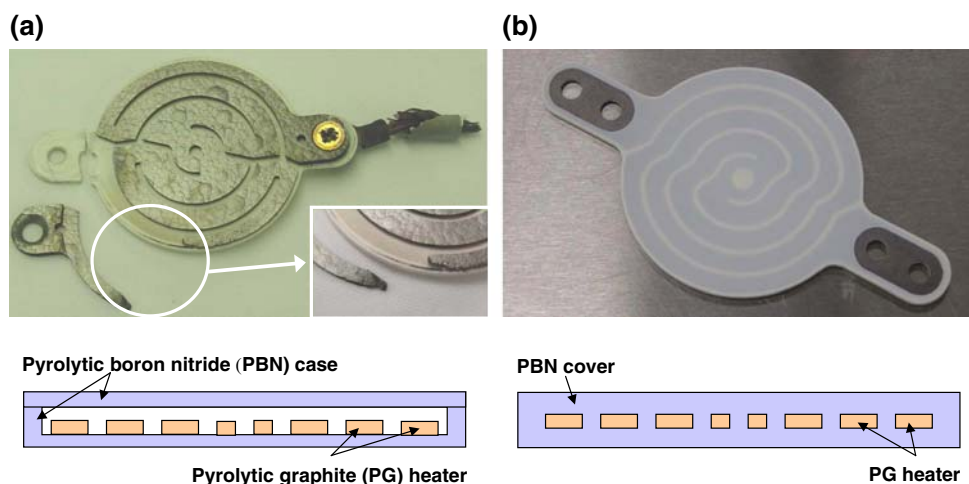


Fig. 3 Photographs and cross-sectional structures of: **a** a damaged PG heater by mechanical stress and **b** an exchanged PG/PBN heater

was important we developed a control software for ultrasonic-NIL system that could trigger the onset of the ultrasonic vibration automatically when a loading force reaches a prescribed marker or set pushing depth.

2.2 Fabrication of Si mold by MEMS fabrication technologies

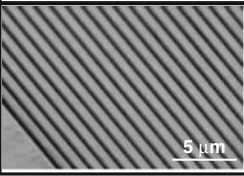
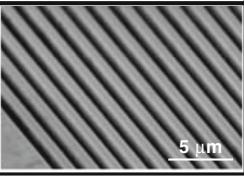
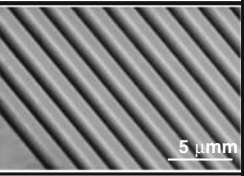
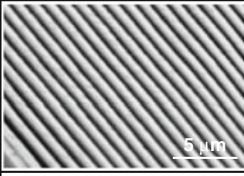
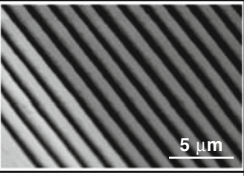
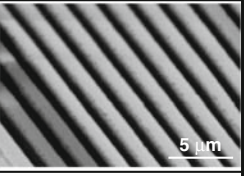
In nanoimprint experiments, a concave-type Si mold was used where features of its patterns were defined by: depth = 3 μm , length = 1.8 μm , and line widths = 500, 750 nm, and 1 μm . The Si mold was fabricated according to the procedures described here. At first, a 400 nm thick film of an electron beam (EB) positive-type resist (ZEP520A, Zeon Corp.) was spin-coated on a 400- μm thick Si wafer. A pattern was transcribed by using an EB lithography system (ELS-7700H, Elionix Co., Ltd) after a pre-bake; the wafer was then developed after post exposure bake. The Si wafer was etched down to a depth of 3 μm with an reactive-ion-etching (RIE) system (Alcatel 601E, Alcatel Vacuum Technology France) where the EB resist pattern acted as a masking layer during the etch. The EB resist was removed by O_2 plasma ashing with another RIE system (Model RIE-10NRS, Samco Inc.). SEM images of Si mold patterns are shown in the upper row of Table 1. The Si trench structure with 3 μm high vertical sidewall was processed by optimizing the etching condition. The Si mold size was 10 mm square.

3 Experiments and discussion

3.1 Experimental procedure

Figure 4 shows the experimental procedures of the thermal-NIL and the ultrasonic-NIL. A rubber sheet in the thickness of 3 mm was put on the bottom loading stage, and it was then covered with a Teflon sheet in the thickness of 50 μm . For a molding material we selected PC which also has high demand as a material for optical device. The glass transition temperature of PC is 150°C. A 10 mm square PC sheet in the thickness of 0.5 μm was put on the Teflon sheet, and a Si mold was set on it. The pattern side of the Si mold faced the PC sheet where the two could come into direct contacts with each other. For an easy flake off after imprinting, a release agent (EGC-1720, Sumitomo 3M Ltd.) was spread on the pattern side of the Si mold. After the setup, the upper loading stage was heated to a pre-set temperature. Next, the upper loading stage was moved downward along the Z axis, and brought close to the Si mold, where the Si mold could be heated by radiation. The upper loading stage was brought close to the mold where the gap between the upper loading stage and the Si mold became 1 mm or less. After maintaining at this position for 5 min the upper loading stage was lowered further down where the Si mold could be pressed against the PC sheet with a pre-determined contact force. After the contact force was set at a pre-determined force it was maintained there for 10 or 60 s.

Table 1 SEM images of nano-patterns of Si mold and PC imprinted by thermal-NIL

Line width		500 nm	750 nm	1 μm
Si mold	SEM images			
	height	2.78 μm	2.69 μm	3.02 μm
PC patterns imprinted at 180 °C	SEM images			
	height	0.53 μm	0.69 μm	1.18 μm

After that, the upper loading stage was cooled down to 130°C, and was then pulled back to its original position along the Z axis. In the case of ultrasonic-NIL experiments, on the other hand, an ultrasonic vibration of longitudinal wave was also generated while applying the load, as shown in Fig. 4b. The ultrasonic vibration was stopped at the same time when the cooling process was started where the upper loading stage was cooled down to 130°C. After the upper loading stage had been raised, the Si mold was peeled off from the solidified PC sheet by the hand.

3.2 Preliminary experiment without using ultrasonic vibration

In hot embossing experiments of PC, the optimized mold heating temperature was 180°C (Mekaru et al. 2007). As a part of our experiment the above technique was then extended to thermal NIL where the experiment was executed using the same conditions (heating temperature: 180°C, contact force: 100 N, and contact time: 10 s). SEM images of imprinted patterns with line width of 500, 750 nm, and 1 μm are shown in middle row of Table 1.

Fig. 4 Experimental procedure of: **a** thermal-NIL and **b** ultrasonic-NIL

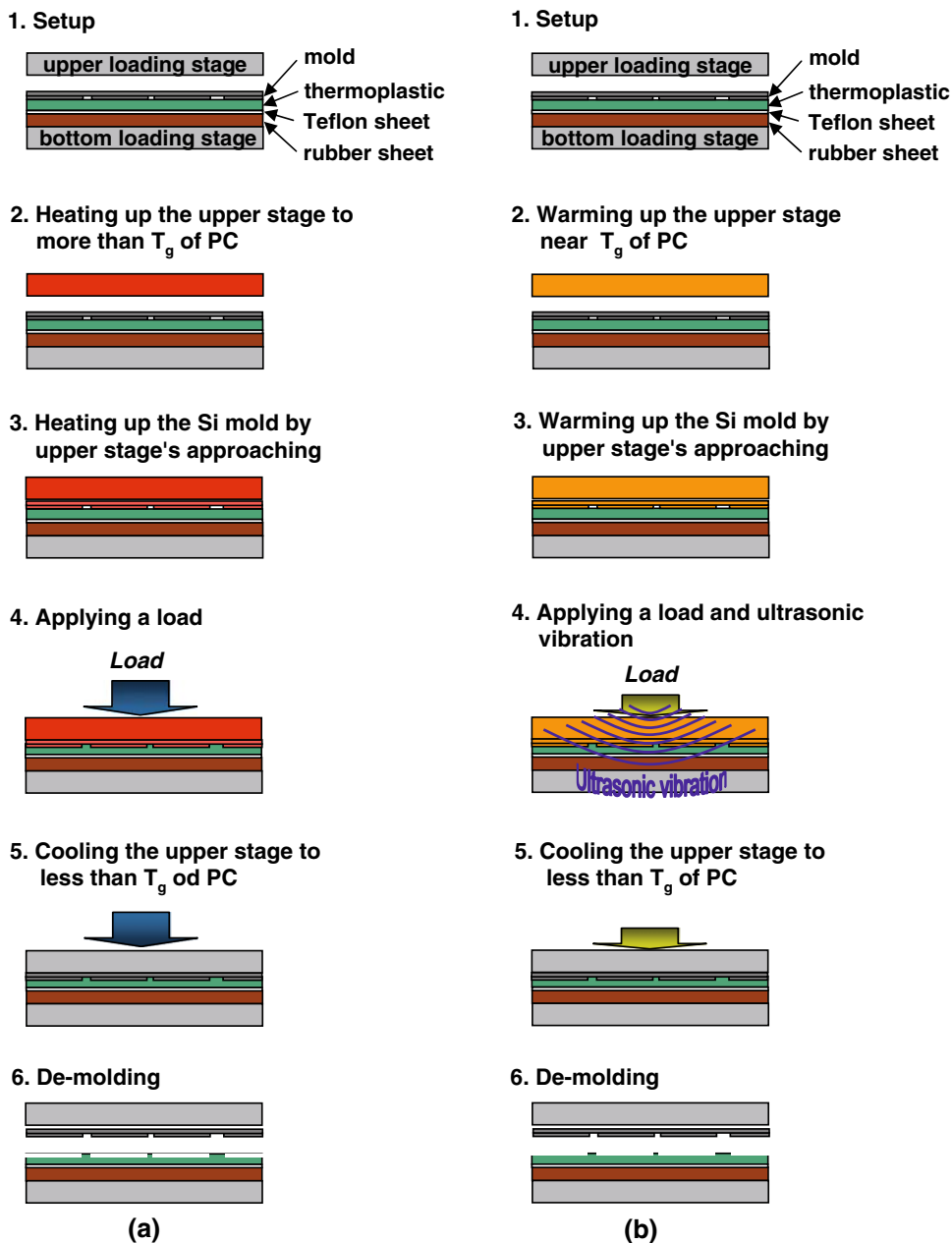


Table 2 SEM images of PC imprinted patterns in ultrasonic-NIL with high amplitude

	Line width		
	500 nm	750 nm	1 μm
Point I			
Point II			
Point III			
Point IV			
Point V			

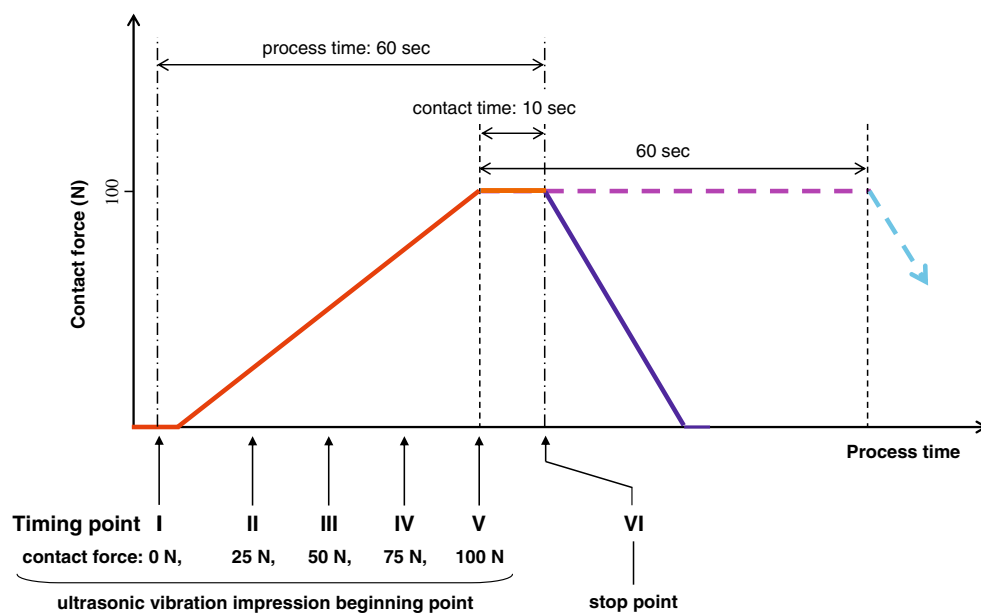
The heights of imprinted patterns were measured with a 3D optical profiler (NewView 5000, Zygo Corp.). The PC pattern with a maximum aspect ratio of 5.56 ($=2.78 \mu\text{m}/500 \text{ nm}$) could be imprinted. However, the thickness of the PC sheet that was originally 0.5 mm had thinned down to 0.27 mm. So as not to transform the PC sheet as much as possible, the mold heating temperature was reduced to 150°C; this happens to be the same as that of the glass

transition temperature of PC. The lower row in Table 1 shows SEM images of imprinted patterns with line widths of 500, 700 nm, and 1 μm with this condition. A large difference appeared to the molding accuracy when the mold heating temperature was 180°C. The maximum height of the imprinted pattern was 1.18 μm , and the highest aspect ratio was 1.06 ($=0.53 \mu\text{m}/500 \text{ nm}$) in the case that the line width was 1 μm . As compared with when the mold heating temperature was 180°C, the highest aspect ratio had decreased to one-fifth of its original value.

3.3 Effect of assistance of ultrasonic vibration in thermal-NIL

Ultrasonic-NIL experiments were executed based on the result of the preliminary experiment. The parameters for the experiment were fixed as the following: mold heating temperature = 150°C; contact force = 100 N, and the contact time = 10 s. These numbers point out that the experiment was done at a temperature below the glass transition temperature of PC. Figure 5 shows the relationships between the process time and the contact force. Timings I–V in the Fig. 5 indicates starting points of the ultrasonic vibration impression. Timing VI in the same figure indicates the stopping point for all ultrasonic vibration. The first impression marked by I denotes that the timing of the ultrasonic vibration began when the contact force was 0 N. In other words, it was the case where the ultrasonic vibration impression began before the Si mold even touched the PC sheet. The timings markers II, III, IV, and V point out the times where the ultrasonic vibration impression began after the contact force reached

Fig. 5 Relation between timing points of applying ultrasonic vibration and contact force



the points 25, 50, 75, and 100 N, respectively. All the ultrasonic vibrations were stopped according to the timing VI after contacting for 10 s. The speed of the press and the release was 1.0 $\mu\text{m/s}$. Fifty seconds were required from the time Si mold made its initial contact with the PC sheet (contact force ~ 0 N) to the time when the contact force reached its maximum value of 100 N. SEM images of PC patterns imprinted under these conditions, with line widths of 500, 750 nm, and 1 μm , are shown in Tables 2 and 3. These are the experimental results from the cases where the amplitude of the ultrasonic vibration was 1.8 μm (high-mode level 5) and 1.25 μm (low-mode level 5), and are shown in Tables 2 and 3, respectively. Points I–V in the left column in Tables 2 and 3 show timings at which each ultrasonic vibration impression was started in Fig. 5. When the ultrasonic vibration of the maximum amplitude 1.8 μm was impressed (Table 2), it can be observed that imprinted patterns is shape near the imprinted pattern of the middle row as compared with the lower row in Table 1. This phenomenon can be clearly confirmed in Fig. 6 where the measurement results of the heights of the imprinted pattern are shown. Especially, the application of the ultrasonic vibration according to early timing seemed to improve the molding accuracy. Heights of the imprinted pattern of all line widths showed a rise when the impression of the ultrasonic vibration began with timings I (contact force = 0 N) and II (contact force = 25 N), as compared with the case where we did not apply the ultrasonic vibration. Even when the impression of the

Table 3 SEM images of PC imprinted patterns in ultrasonic-NIL with low amplitude

	Line width		
	500 nm	750 nm	1 μm
Point I			
Point II			
Point III			
Point IV			
Point V			

ultrasonic vibration began with other timings, any substantial change was not confirmed in the pattern with line widths 750 nm and 1 μm though the height of the imprinted pattern with the line width of 500 nm showed a

Fig. 6 Height of PC imprinted patterns in ultrasonic-NIL with high amplitude

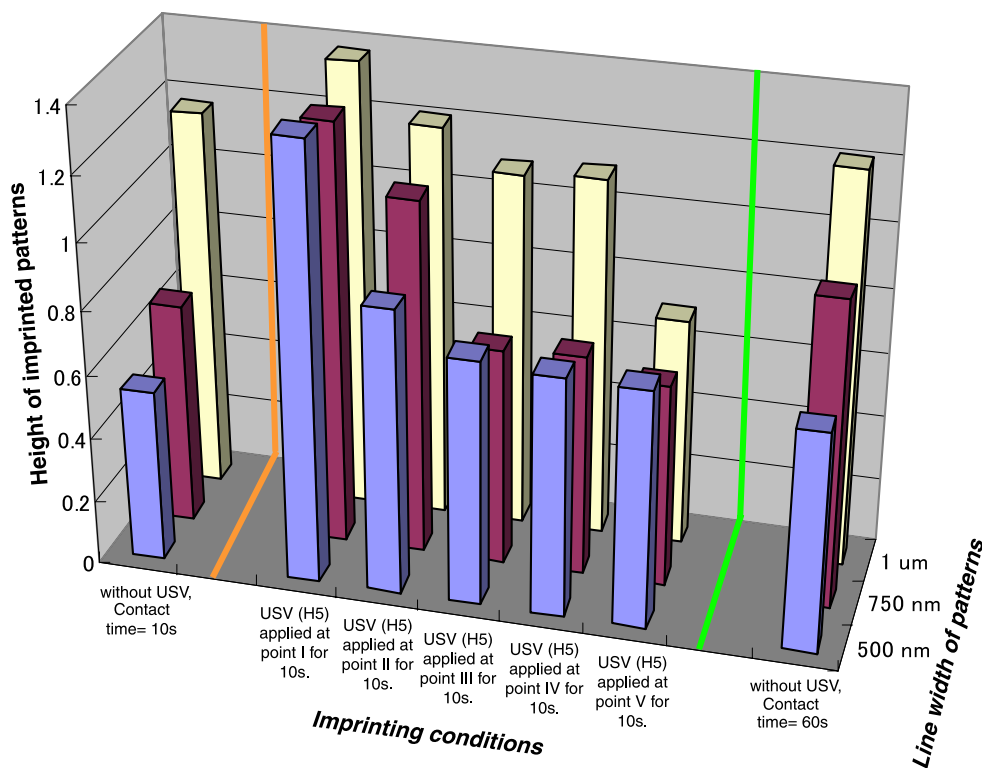
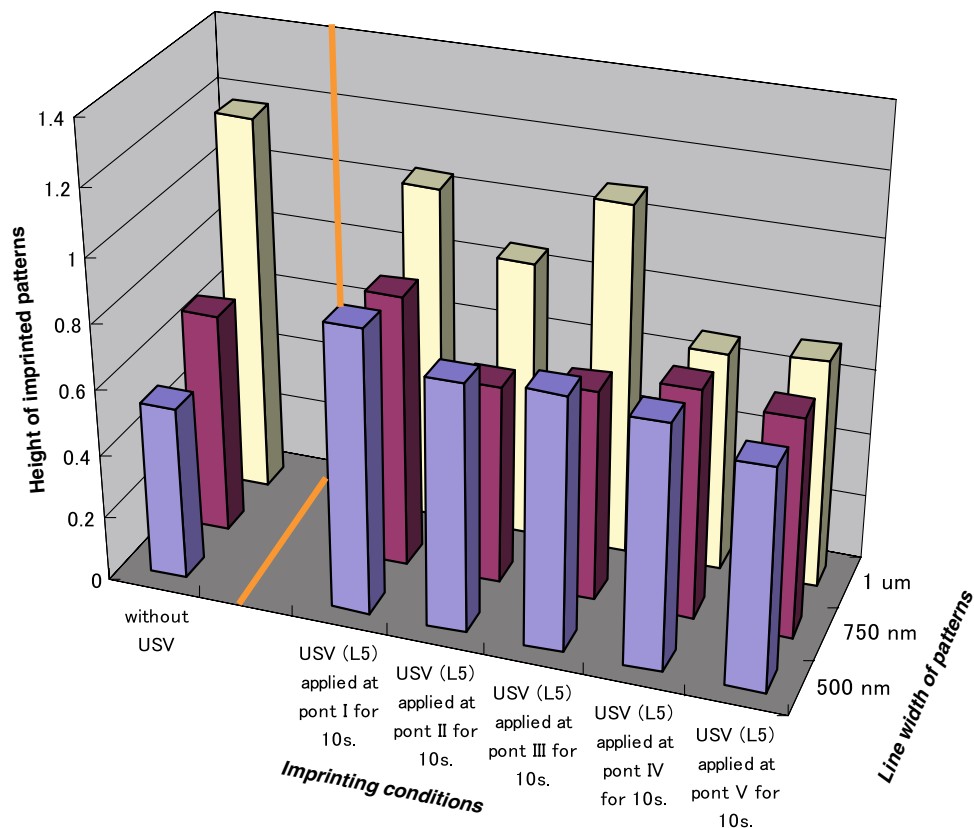


Fig. 7 Height of PC imprinted patterns in ultrasonic-NIL with low amplitude



rise. Moreover, when the impression of the ultrasonic vibration began on the timing I, the ultrasonic vibration had been continuously impressing for 60 s. Though the contact time was extended to 60 s without applying the ultrasonic vibration as shown by the dotted line in Fig. 5 for the confirmation, a noticeable increase in the height of the imprinted pattern was not observed.

When the ultrasonic vibration in the maximum amplitude of $1.25 \mu\text{m}$ was impressed (Table 3), the molding accuracy of imprinted patterns was the same level as the lower in Table 1 or less. This phenomenon can be obviously confirmed even by the measurement results of the height of the imprinted pattern shown in Fig. 7. A dramatic increase in the height of the imprinted pattern by the difference of timing in which the impression of the ultrasonic vibration began was not seen compared with case of the maximum amplitude of $1.8 \mu\text{m}$. In the case of the line width of 500 nm, the height of patterns with impressing the ultrasonic vibration increased compared with the case where the ultrasonic vibration was not impressed. In the case of the line width of 750 nm, it was confirmed that the height of the pattern increased where the impressing of the ultrasonic vibration started at the timing I (contact force = 0 N). Such a phenomenon shows that the flowing of the thermoplastic cannot be assisted enough by the ultrasonic vibration with low amplitude.

4 Summary

We have developed an ultrasonic-NIL system that can apply the ultrasonic vibration, thermal stress, and loading force into the molding process. To overcome the mechanical stress by the ultrasonic vibration, a PG/PBN all-in-one design heater was built into the upper loading stage of the system. We learned that in order to manage and manipulate the timing at which the ultrasonic vibration can be impressed is needed, the program for controlling the ultrasonic vibration generation device was improved. Using the system, ultrasonic nanoimprinting of PC was carried out at 150°C , which is the glass transition temperature of PC. We learned that the amplitude of the ultrasonic vibration and the start times of the impressions of ultrasonic vibration were important molding conditions that determined the quality of nanoimprints. As for the start time of the impression of the ultrasonic vibration set at an earlier stage in the molding process, the effect of assistance of the ultrasonic vibration was significant. Especially in the case where the impressions of the ultrasonic vibration began before the upper loading stage came into contact with the Si mold, the molding accuracy was found to have improved and the height of imprinted patterns increased. In addition, there was found an important relationship between the aspect ratio of the imprinted pattern and the

amplitude of the ultrasonic vibration in the ultrasonic-NIL. Thus, the effect of assistance of the ultrasonic vibration exhibited remarkable contribution to the molding technology applied in the area of nano-field.

References

- Becker EW, Ehrfeld W, Hagmann P, Maner A, Münchmeyer D (1986) Fabrication of microstructures with high aspect ratios and great structural heights by synchrotron radiation lithography, galvanofarming, and plastic moulding (LIGA process). *Microelectron Eng* 4:35–42
- Chou SY, Krauss PR, Renstrom PJ (1995) Imprint of sub-25 nm vias and trenches in polymers. *Appl Phys Lett* 67:3114–3116
- Kishi H, Yoshioka H, Jianguo Y, Sumiyoshi N, Goto H, Murakoshi Y, Maeda R (2003) Thermal imprinting stepper with ultrasonic vibration mechanism and rapid temperature control system. *Proceedings of second international conference on nanoimprint nanoprnt technology: B6, Boston, 3–5 Dec 2003*
- Lorenz H, Despont M, Vettiger P, Renaud P (1998) Fabrication of photoplastic high-aspect ratio microparts using SU-8 UV resist. *Microelectron Eng* 4:143–146
- Maeda R, Ashida K (2004) Mechanical lithography—state of the art and the future. *J Jpn Soc Precis Eng* 70:1219–1222 (in Japanese)
- Mekaru H, Nakamura O, Maruyama O, Maeda R, Hattori T (2007) Development of precision transfer technology of atmospheric hot embossing by ultrasonic vibration. *Microsyst Technol* 13:385–391
- Mekaru H, Goto H, Takahashi M (2006) Development of ultrasonic micro hot embossing technology. *Microelectron Eng* 84:1282–1287